PLOS | COMPUTATIONAL BIOLOGY

RESEARCH ARTICLE

Reduction of multiscale stochastic biochemical reaction networks using exact moment derivation

Jae Kyoung Kim[1☯]*, **Eduardo D. Sontag**[2☯]*

1 Department of Mathematical Sciences, Korea Advanced Institute of Science and Technology, Daejeon, Korea, **2** Department of Mathematics and Center for Quantitative Biology, Rutgers University, New Brunswick, New Jersey, United States of America

☯ These authors contributed equally to this work.
* jaekkim@kaist.ac.kr (JKK); eduardo.sontag@rutgers.edu, eduardo.sontag@gmail.com (EDS)

Citation: Kim JK, Sontag ED (2017) Reduction of multiscale stochastic biochemical reaction networks using exact moment derivation. PLoS Comput Biol 13(6): e1005571. https://doi.org/10.1371/journal.pcbi.1005571

Editor: Lingchong You, Duke University, UNITED STATES

Received: February 13, 2017

Accepted: May 12, 2017

Published: June 5, 2017

Data Availability Statement: Code is available at https://github.com/jaekkim/feedme.

Funding: This work was supported by: National Research Foundation of Korea grant N01160447, http://www.nrf.re.kr/index, to JKK; TJ Park Science Fellowship of POSCO TJ Park Foundation, https://www.postf.org/ko/main.do, to JKK; US Office of Naval Research grant ONR N00014-13-1-0074, https://www.onr.navy.mil/contracts-grants.aspx to EDS; US Air Force Office of Scientific research grant AFOSR FA9550-14-1-0060, http://www.wpafb.af.mil/afrl/afosr, to EDS. The funders had no

Abstract

Biochemical reaction networks (BRNs) in a cell frequently consist of reactions with disparate timescales. The stochastic simulations of such multiscale BRNs are prohibitively slow due to high computational cost for the simulations of fast reactions. One way to resolve this problem uses the fact that fast species regulated by fast reactions quickly equilibrate to their stationary distribution while slow species are unlikely to be changed. Thus, on a slow timescale, fast species can be replaced by their quasi-steady state (QSS): their stationary conditional expectation values for given slow species. As the QSS are determined solely by the state of slow species, such replacement leads to a reduced model, where fast species are eliminated. However, it is challenging to derive the QSS in the presence of nonlinear reactions. While various approximation schemes for the QSS have been developed, they often lead to considerable errors. Here, we propose two classes of multiscale BRNs which can be reduced by deriving an exact QSS rather than approximations. Specifically, if fast species constitute either a feedforward network or a complex balanced network, the reduced model based on the exact QSS can be derived. Such BRNs are frequently observed in a cell as the feedforward network is one of fundamental motifs of gene or protein regulatory networks. Furthermore, complex balanced networks also include various types of fast reversible bindings such as bindings between transcriptional factors and gene regulatory sites. The reduced models based on exact QSS, which can be calculated by the computational packages provided in this work, accurately approximate the slow scale dynamics of the original full model with much lower computational cost.

Author summary

Molecules inside a cell undergo various transformations via biochemical reactions with disparate rates. For instance, while transcriptional factors bind and unbind gene promoters in a time scale of seconds, mRNA transcription takes at least several minutes. For such systems regulated by both fast and slow reactions together, most of the computation time

role in study design, data collection and analysis, decision to publish, or preparation of the manuscript.

Competing interests: The authors have declared that no competing interests exist.

in stochastic simulations is spent on simulating the fast reactions, even if our interest is in the dynamics of slow reactions such as transcription. This problem can be resolved by deriving a reduced system, which can accurately approximate the slow dynamics of the original system without simulating fast reactions. However, when nonlinear reactions exist, the accurate reduction is often impossible. Here, we describe that two classes of nonlinear systems, both of which appear frequently as models of natural biochemical reaction networks, can be effectively reduced, and we provide a computational package to carry out the reduction. We find that the resulting reduced systems accurately capture the stochastic dynamics of the original system, while saving considerable simulation time.

Introduction

Many biochemical reaction networks (BRNs) in a cell include species whose copy numbers are small [1–3] (e.g. one or a few copies of genes or tens of mRNAs), which lead to large fluctuations in the system. Such stochastic dynamics of BRNs can be described by the chemical master equation (CME), but the analytic solutions of the CME cannot be calculated in most cases. Thus, to obtain numerical solutions of the CME, the Gillespie algorithm has been widely used, which generates exact sample paths of the CME [4]. However, such numerical simulation becomes extremely inefficient in the presence of stochastic stiffness [5, 6]. Specifically, in the presence of fast reactions, stochastic simulations become slow as the computation is predominantly spent on simulating fast reactions. Thus, it becomes computationally prohibitive to use the Gillespie algorithm to simulate multiscale BRNs.

One approach to resolve this problem is utilizing timescale separation among species in multiscale BRNs [7–13]. In such networks, fast species regulated by fast reactions will quickly equilibrate to their stationary distributions while slow species remain constant. Thus, on the slow timescale, the fast species in propensity functions of reactions rapidly average out to their quasi-steady-state (QSS): their stationary conditional expectation value for given states of slow species. As the QSS is solely determined by the state of slow species, replacement of the fast species with their QSS leads to a reduced model, where fast species are eliminated. This reduced system accurately captures the dynamics of slow species of the original full system on the slow timescale without simulating fast species and thus with much lower computational cost.

In the presence of nonlinear reactions, moment equations usually involve infinite ODEs and thus deriving the exact QSS becomes challenging. Thus, various approximations for QSS have been proposed [8, 14–27]. However, the validity conditions have often been tested with some toy examples and thus general validity conditions of such approximations have not been fully understood. For instance, a popular approximation is using the QSS of the corresponding deterministic system (e.g. large volume limit of the stochastic system) [8, 21–23]. Specifically, deterministically derived QSS such as Michaelis-Menten and Hill functions has been used to approximate the stochastic QSS and derive the propensity functions of the Gillespie algorithm. Despite the popularity of this approach [28–44], it can lead to considerable errors depending on the parameter choice [9, 45–51]. Furthermore, its validity conditions have been investigated only recently [45–51] and have not been fully identified yet for general cases.

Despite the difficulty in the derivation of the exact QSS in general, recent studies have revealed that such derivations are possible for several special cases of nonlinear BRNs (see [52] for a recent review for this topic). Stationary solutions of CMEs associated to enzyme kinetics have been studied in [53–55]. In particular, Levine and Hwa used the exact QSS of an enzyme

kinetics system to reduce various types of models that appear in metabolic pathways [56]. Furthermore, the stationary distribution for a single gene regulatory model was also derived recently [57–59].

In this work, rather than focusing on a specific case, we investigate the exact QSS of two general classes of nonlinear BRNs, which are frequently found in many natural biological systems. The first class is BRNs whose fast subnetwork is a feedforward network. In contrast to linear systems, moment equations of nonlinear systems depend on higher orders, and lead in general to an infinite system of coupled ODEs. However, in the recent work [60], Sontag and Singh proved that all moments of a certain class of nonlinear feedforward networks can be computed by finite linear differential equations. We will describe how this theory can be used to derive an accurate reduction of a nonlinear BRN whose fast subnetwork is a feedforward network. To aid in implementations, we provide a computational package, FEEDME, which calculates the moments of interest for systems with a linear moment closure property and thus the exact QSS of the embedded feedforward network.

In [61], Anderson, Craciun, and Kurtz showed how stationary distributions of a certain broad class of BRNs, namely complex balanced networks, have the form of a multivariate Poisson distribution normalized by an appropriate partition function which accounts for conservation laws; they then applied their result to several examples, including a model of multiscale enzyme kinetics. The key difficulty in obtaining the stationary distribution and thus stationary moments becomes then to compute this partition function. In [62], Sontag and Zeilberger developed an approach, based on transforms and factorial moments, to compute this function as well as all first and higher-order moments, for complex balanced networks. Moreover, Wilf-Zeilberger theory led to a formula that computes the partition function recursively on integer conserved amounts (see Methods for details on the basic theorems from [61] and [62]). The applicability of these results for the model reduction was not studied in [62], however. Recently, Mélykúti, Hespanha, and Khammash in [63] derived analytic expressions for an extensive collection of nonlinear BRNs, including reversible bindings on path-like, circular, and ladder-shaped state spaces, also framing the discussion in the context of complex balancing, and explained how those results can be used in model reduction, but [63] did not take advantage of the methods and formulas in the paper [62] which provide a general theoretical and algorithmic approach in the complex balanced case. In the present paper, we make full use of the theory in [62] in order to effectively derive an exact QSS for complex balanced networks. This provides a systematic way to perform the time-scale reduction for the second class of BRNs, those whose fast subnetwork constitutes a complex balanced network.

We illustrate the procedure of QSS derivation, and thus reduction, for both classes of systems with several examples, including a transcriptional negative feedback loop combined with a fast feedforward signaling pathway, a genetic oscillator with a fast reversible binding and a transcriptional positive feedback loop with fast competitive reversible bindings. In every case, we show how the reduced models based on the exact QSS outperform those based on the approximate QSS.

Results

Reduction of a multiscale feedforward network

Feedforward networks are frequently observed in gene and protein regulatory networks as they play the critical roles in response of system for given signals [64, 65]. In the class of feedforward networks considered in this work, species can be partitioned into a series of layers so that every nonlinear reaction among multimers lead to the production of a new species in later layers without destruction of multimers (see Methods for details). Importantly, such

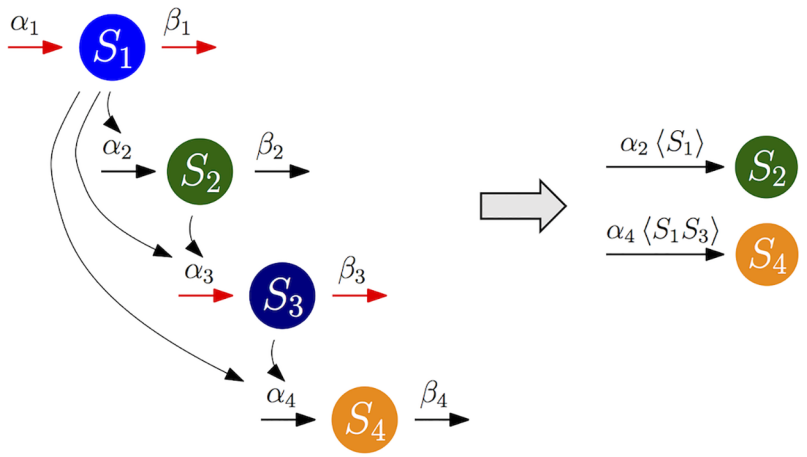

Fig 1. Model diagram of the feedforward network of the full model and the reduced model. In the diagram of the full model (left), red arrows indicate fast reactions. In the diagram of the reduced model (right), which consists of slow species S_2 and S_4 and slow reactions, $\langle S_1 \rangle$ and $\langle S_1 S_3 \rangle$ represent conditional moments, $\langle X_1 | X_2, X_4 \rangle$ and $\langle X_1 X_3 | X_2, X_4 \rangle$, respectively. In both of the diagrams, degradation reactions are not shown, for simplicity.

https://doi.org/10.1371/journal.pcbi.1005571.g001

feedforward networks have the linear moment closure property, and thus any of their moments can be calculated using Eq (15) recursively even in the presence of nonlinear reactions [60]. Our algorithm, FEEDME, uses such a property to calculate moments of interest. In particular, the stationary conditional moments of fast species given slow species can be derived, which allows for accurate reductions of multiscale stochastic systems.

Here, we illustrate this reduction process using an example of multiscale nonlinear feedforward network (Fig 1). This system consists of 4 species and 8 reactions (Table 1): S_1 is constitutively produced. S_1, a heterodimer consisting of S_1 and S_2, and a heterodimer consisting of S_1 and S_3 promote the production of S_2, S_3, and S_4, respectively. S_i degrades with its own rate. Propensity functions are derived based on mass action kinetics by defining $X_i(t)$ be the abundance of the species S_i at time t (Table 1).

As reactions involving the synthesis and degradation of S_1 and S_3 are faster than other reactions (Fig 1 and Table 1), S_1 and S_3 are fast species that rapidly fluctuate and quickly equilibrate to their stationary distribution conditioned on the slow species. Thus,

Table 1. Reactions and propensity functions in the feedforward network (Fig 1).

Reactions	Propensity functions
$\xrightarrow{\alpha_1} S_1$	$\alpha_1 \Omega$
$S_1 \xrightarrow{\beta_1}$	$\beta_1 X_1$
$S_1 \xrightarrow{\alpha_2} S_1 + S_2$	$\alpha_2 X_1$
$S_2 \xrightarrow{\beta_2}$	$\beta_2 X_2$
$S_1 + S_2 \xrightarrow{\alpha_3} S_1 + S_2 + S_3$	$\frac{\alpha_3}{\Omega} X_1 X_2$
$S_3 \xrightarrow{\beta_3}$	$\beta_3 X_3$
$S_1 + S_3 \xrightarrow{\alpha_4} S_1 + S_3 + S_4$	$\frac{\alpha_4}{\Omega} X_1 X_3$
$S_4 \xrightarrow{\beta_4}$	$\beta_4 X_4$

Here, $\alpha_1 \Omega = 2/\epsilon\ m^{-1}$, $\alpha_3/\Omega = 2/\epsilon\ m^{-1}$, $\alpha_2 = 2\ m^{-1}$, $\alpha_4/\Omega = 2\ m^{-1}$, $\beta_1 = \beta_3 = 1/\epsilon\ m^{-1}$, and $\beta_2 = \beta_4 = 1\ m^{-1}$. Ω represents the volume of the system and $\epsilon \ll 1$.

https://doi.org/10.1371/journal.pcbi.1005571.t001

the propensity functions of slow reactions involving fast species, $\alpha_2 X_1$ and $(\alpha_4/\Omega)X_1X_3$, rapidly equilibrate to their stationary conditional expectation values, $\alpha_2\langle X_1|X_2, X_4\rangle$ and $(\alpha_4/\Omega)\ \langle X_1X_3|X_2, X_4\rangle$, respectively. Our algorithm, FEEDME, allows for calculating these moments in terms of slow species:

$$\alpha_2\langle X_1|X_2, X_4\rangle \quad = \quad \frac{\alpha_1\alpha_2\Omega}{\beta_1}, \tag{1}$$

$$\alpha_4/\Omega\langle X_1X_3|X_2, X_4\rangle \quad = \quad \alpha_4 X_2\left(\frac{\alpha_1^2\alpha_3}{\beta_1^2\beta_3}+\frac{\alpha_1\alpha_3}{(\beta_1+\beta_3)\beta_1\Omega}\right). \tag{2}$$

By substituting these QSS for the original propensity functions, we can derive a reduced system, which solely consists of slow species S_2 and S_4 (Fig 1). We refer to this reduced model as the EMB model (exact-moment based model) for this example. When such exact moments cannot be calculated, an alternative popular approach uses the deterministically derived QSS under the moment closure assumption ($\langle X_iX_j\rangle = \langle X_i\rangle\langle X_j\rangle$) [8, 21–23] as follows:

$$\alpha_4/\Omega_1\langle X_1X_3|X_2, X_4\rangle \approx \alpha_4/\Omega\langle X_1|X_2, X_4\rangle\langle X_3|X_2, X_4\rangle = \alpha_4 X_2\left(\frac{\alpha_1^2\alpha_3}{\beta_1^2\beta_3}\right). \tag{3}$$

Note that this approximate moment is the limit of the exact moment Eq (2) as $\Omega\rightarrow\infty$ (i.e. as one gets closer to the deterministic system). We refer to the reduced model based on this approximate moment as the AMB model (approximate-moment based model) for this example.

We compared the stochastic simulations of the full model with $\epsilon = 0.01$, the EMB model and the AMB model. The mean and standard deviation of simulated trajectories of the full model is accurately captured by the EMB model (Fig 2A), but not by the AMB model (Fig 2B). In addition, as ϵ decreases, both the mean and the standard deviation of S_4 at the steady state of the full model approach those of the EMB model (Fig 2C), but not those of the AMB model (Fig 2D). This indicates that the stochastic reduction based on exact moments is accurate as long as there is a large enough timescale separation. This is consistent with previous theoretical studies [8, 26]. Furthermore, note that as ϵ decreases, not only does the accuracy of the EMB model increase, but also a longer computation time would be required for the simulation of the full model, rendering even more clear the benefit of our reduction. Taken together, these results provide evidence that our algorithm, FEEDME, allows for accurate stochastic reductions for mutli-scale feedforward networks.

Next, we illustrate how a key property of the original full model can be revealed only by the EMB model, but not by the AMB model. In the feedforward network that we study, a critical issue is understanding the relationship between input molecules (S_1) and downstream output molecules (S_4). Suppose that the production rate (α_1) and the degradation rate (β_1) of S_1 change proportionally, which ensures that the average copy number of S_1 is invariant. A natural question is: do the average copy number and the fluctuation level of S_4 change? From Eq (3), the stationary average number of S_4 in the AMB model can be derived as follows:

$$\langle X_4\rangle = \frac{\alpha_4}{\beta_4}\langle X_2\rangle\left(\frac{\alpha_1^2\alpha_3}{\beta_1^2\beta_3}\right) = \Omega\left(\frac{\alpha_1}{\beta_1}\right)^3\frac{\alpha_2\alpha_3\alpha_4}{\beta_2\beta_3\beta_4}, \tag{4}$$

which predicts that $\langle X_4\rangle$ does not change as long as $\frac{\alpha_1}{\beta_1}$ and thus $\langle X_1\rangle = \Omega\frac{\alpha_1}{\beta_1}$ are maintained. However, the stationary average number of S_4 derived with the EMB model using Eq (2) leads

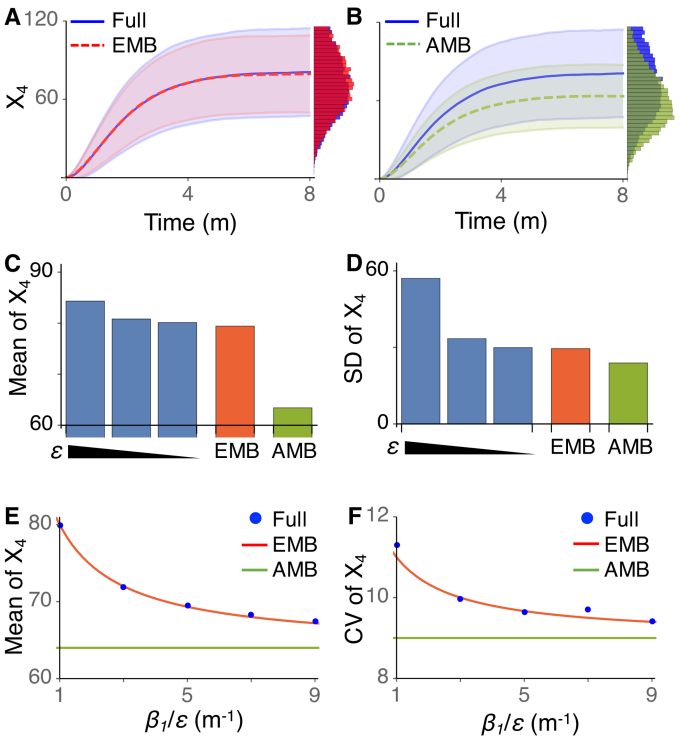

Fig 2. EMB model provides much more accurate approximation of the original feedforward network model than AMB model. (A-B) Trajectories of original full model with $\epsilon = 0.01$ and the EMB model (A) and the AMB model (B). The lines and colored ranges indicate the mean of X_4 and standard deviations of X_4 from their mean, respectively. Histograms represent distributions of X_4 at the steady state. Here, $X_1(0) = \alpha_1/\beta_1$, $X_2(0) = X_3(0) = X_4(0) = 0$. Here, 10^4 stochastic simulations were performed. (C-D) Mean (C) and standard deviation (D) of stationary distribution (t = 8) simulated with the full model with varying $\epsilon = 0.1, 0.05, 0.01$, the EMB model and the AMB model. (E-F) As $\beta_1 = \alpha_1$ increases, the EMB model, but not the AMB model, predicts that the mean and the CV of S_4 decrease, which is consistent with the simulations of the original full model.

https://doi.org/10.1371/journal.pcbi.1005571.g002

to a different conclusion, namely:

$$\langle X_4\rangle = \frac{\alpha_4}{\beta_4}\langle X_2\rangle\left(\frac{\alpha_1^2\alpha_3}{\beta_1^2\beta_3}+\frac{\alpha_1\alpha_3}{(\beta_1+\beta_3)\beta_1\Omega}\right) = \Omega\left(\frac{\alpha_1}{\beta_1}\right)^3\frac{\alpha_2\alpha_3\alpha_4}{\beta_2\beta_3\beta_4}+\left(\frac{\alpha_1}{\beta_1}\right)^2\frac{\alpha_2\alpha_4}{\beta_2\beta_4}\frac{\alpha_3}{(\beta_1+\beta_3)}, \quad (5)$$

which decreases even when α_1 and β_1 increase proportionally. This is consistent with the simulation of the full model (Fig 2E). Furthermore, as, in contrast to the original full model, the AMB and the EMB model are linear, the coefficient of variation of S_4 in both the AMB and the EMB model can be easily derived, and it is

$$1+\frac{\langle X_4\rangle}{\langle X_2\rangle}\frac{1}{1+\beta_2/\beta_4}.$$

In the AMB model, $\langle X_4\rangle$ does not change, as long as $\langle X_1\rangle$ is maintained constant, and thus the C.V. of S_4 remains constant. On the other hand, the C.V. of S_4 in the EMB model decreases even when $\langle X_1\rangle$ is maintained constant due to a proportional increase in its production and degradation rate, a behavior which is also consistent with the full model (Fig 2F). Taken together, these two observations show that EMB model, but not the AMB model, can accurately capture an important feature of the original full model, namely that average copy number and fluctuation level of the output molecule (e.g. S_4) in the feedforward loop depends both

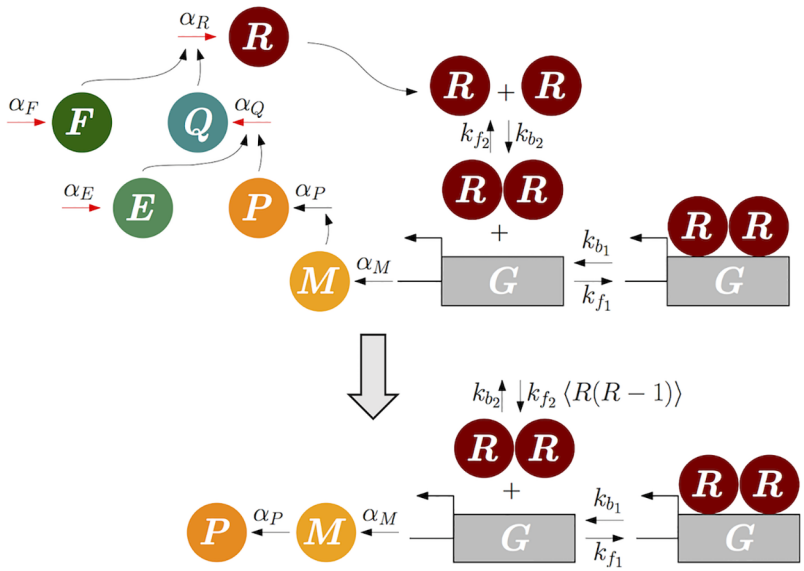

Fig 3. Model diagram of a transcriptional negative feedback loop with a fast feedfoward subnetwork and a slow dimerization. In the diagram of the full model (top), red arrows indicate fast reactions. Note that the subnetwork consisting of the fast species *E*, *Q*, *F*, and *R* with fast reactions (red arrows) is feedforward. In the diagram of the reduced model (bottom), which solely consists of slow species and slow reactions, $\langle R(R-1)\rangle$ represents a conditional moment, $\langle X_R(X_R-1)|X_P\rangle$. In both of the diagrams, all degradation reactions are not shown, for simplicity.

https://doi.org/10.1371/journal.pcbi.1005571.g003

on the timescale of the input molecule (i.e. S_1) and on its average level. This illustrates the importance of the accurate model reduction and its advantage over the original full model.

Reduction of a multiscale system with an embedded fast feedforward subnetwork

Previously, we illustrated how our algorithm, FEEDME can be used to derive the accurate reduction of the multiscale feedforward network (Fig 1). In fact, FEEDME can be used to obtain an accurate reduction of more general BRNs. For the reduction, calculation of all the moments is not necessary, and knowing the conditional moments of certain fast species involved with the slow propensity functions is enough. Thus, as long as the fast subnetwork of the BRN is a feedforward network, the conditional moments of the fast species can be derived with the FEEDME algorithm, and thus an accurate reduction is possible.

We illustrate this case using an example of a transcriptional negative feedback loop with a dimerization (Fig 3). This system consists of 16 reactions including fast feedforward reactions and slow reversible bindings (Table 2): active gene (*G*) promotes the transcription of mRNA (*M*), which is then translated to the protein (*P*). This protein acts as an enzyme which triggers the production of repressor (*R*) via a fast feedforward network, which involves fast species, *Q*, *E* and *F*. Specifically, *E* functions as a cofactor for the protein *P* to be able to promote the production of *Q*. Similarly, *F* also functions as a cofactor for the protein *Q* so that *Q* can promote the production of repressor protein *R*. Then, dimerized *R*: *R* reversibly binds with *G* to form repressed DNA complex (G_R).

Among slow reactions, dimerization of *R* to *R*: *R* depends on the state of fast species *R*. Thus, we need to derive the QSS of the propensity function for the dimerization, $\frac{k_{f_2}}{\Omega}\langle X_R(X_R-1)|X_P\rangle$. This QSS can be derived using the FEEDME algorithm since all fast

Table 2. Reactions and propensity functions in the transcriptional negative feedback loop with a dimerization (Fig 3).

Reactions	Propensity functions
$G + R : R \xrightarrow{k_{f_1}} G_R$	$\frac{k_{f_1}}{\Omega} X_G X_{R:R}$
$G_R \xrightarrow{k_{b_1}} G + R : R$	$k_{b_1} X_{G_R}$
$G \xrightarrow{\alpha_M} G + M$	$\alpha_M X_G$
$M \xrightarrow{\beta_M}$	$\beta_M X_M$
$M \xrightarrow{\alpha_P} M + P$	$\alpha_P X_M$
$P \xrightarrow{\beta_P}$	$\beta_P X_P$
$\xrightarrow{\alpha_E} E$	$\alpha_E \Omega$
$E \xrightarrow{\beta_E}$	$\beta_E X_E$
$E + P \xrightarrow{\alpha_Q} E + P + Q$	$\frac{\alpha_Q}{\Omega} X_E X_P$
$Q \xrightarrow{\beta_Q}$	$\beta_Q X_Q$
$\xrightarrow{\alpha_F} F$	$\alpha_F \Omega$
$F \xrightarrow{\beta_F}$	$\beta_F X_F$
$Q + F \xrightarrow{\alpha_R} Q + F + R$	$\frac{\alpha_R}{\Omega} X_Q X_F$
$R \xrightarrow{\beta_R}$	$\beta_R X_R$
$R + R \xrightarrow{k_{f_2}} R : R$	$\frac{k_{f_2}}{\Omega} X_R (X_R - 1)$
$R : R \xrightarrow{\beta_{R:R}} R + R$	$\beta_{R:R} X_{R:R}$

Here $\alpha_M = \alpha_P = \beta_M = \beta_P = \frac{k_{f_1}}{\Omega} = k_{b_1} = \frac{k_{f_2}}{\Omega} = k_{b_2} = 1\ m^{-1}$ and
$\alpha_E \Omega = \beta_E = \frac{\alpha_Q}{\Omega} = \beta_Q = \alpha_F \Omega = \beta_F = \frac{\alpha_R}{\Omega} = \beta_R = \frac{1}{\epsilon}\ m^{-1}$. Ω represents the volume of the system and $\epsilon \ll 1$.

https://doi.org/10.1371/journal.pcbi.1005571.t002

species, E, Q, F and R constitute a feedforward network (Fig 3):

$$\frac{k_{f_2}}{\Omega} \langle X_R (X_R - 1) | X_P \rangle = k_{f_2} X_P \left(\frac{X_P}{\Omega} + \frac{1}{\Omega} \frac{7X_P/\Omega + 4}{8} + \frac{1}{\Omega^2} \frac{2X_P/\Omega + 3}{9} \right) \tag{6}$$

By substituting this QSS of the propensity function into the original propensity function for the dimerization, we can derive a reduced model (Fig 3 below), which is referred to as the EMB model for this example. On the other hand, the following approximate moment under the moment closure assumption ($\langle X_i X_j \rangle = \langle X_i \rangle \langle X_j \rangle$) can be used:

$$\frac{k_{f_2}}{\Omega} \langle X_R (X_R - 1) | X_P \rangle \approx \frac{k_{f_2}}{\Omega} \langle X_R | X_P \rangle \langle X_R - 1 | X_P \rangle = k_{f_2} X_P \left(\frac{X_P - 1}{\Omega} \right). \tag{7}$$

The reduced model, where the approximate moment is substituted by $\frac{k_{f_2}}{\Omega} \langle X_R (X_R - 1) | X_P \rangle$, is referred to as the AMB model for this example. Again, when $\Omega \to \infty$ and thus the system becomes closer to the deterministic system, the approximate moment Eq (7) and the exact moment Eq (6) become equivalent.

When Ω is instead small, so that the system has large fluctuations, the AMB model fails to approximate the full model with $\epsilon = 0.01$ (Fig 4B). On the other hand, the EMB model provides an accurate approximation (Fig 4A). Specifically, the mean and standard deviation of trajectories of the full model are accurately captured by the EMB model, but not by the AMB model. Furthermore, as ϵ decreases so that the feedforward subnetwork becomes faster, the mean and standard deviation of the slow species R: R at the steady state of the full model converge to those of the EMB model, but not to those of the AMB model (Fig 4C and 4D). Our example

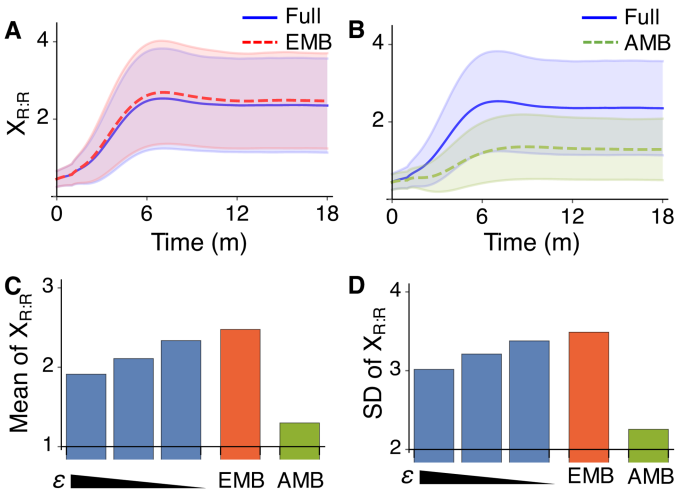

Fig 4. The EMB model provides more accurate approximation of the transcriptional negative feedback loop model than AMB model. (A-B) Trajectories of the full model with $\epsilon = 0.01$ and the EMB model (A) and the AMB model (B). The lines and colored ranges represent $E(X_{R:R})$ and $E(X_{R:R}) \pm SD(X_{R:R})/2$ of 10^4 stochastic simulations. Here $X_i(0) = 0$. (C-D) Mean (C) and standard deviation (D) of steady state distribution of the full model with varying $\epsilon = 0.1, 0.05, 0.01$, the EMB model and the AMB model.

https://doi.org/10.1371/journal.pcbi.1005571.g004

example illustrates how FEEDME can be used to reduce a multiscale BRN whose fast subnetwork is feedforward. In fact, FEEDME can be used for the reduction of more general BRNs as long as their fast subnetwork has a linear moment closure property and thus the QSS can be calculated using Eq (15) recursively.

Reduction of a stochastic system with a fast reversible binding

Next, we consider a different class of multiscale BRNs, those whose fast subnetwork is a complex balanced network. When a network follows mass action kinetics, the network is complex balanced if it is weakly reversible and its deficiency is zero. Weak reversibility means that if there is a path from a given component to another, there is also a reverse (possibly different) path back from the second component to the first one. The deficiency is an integer calculated as the number of components or nodes minus the number of connected components, minus the rank of stoichiometry matrix (see Methods for details). Complex balanced networks can include fast reversible bindings, which are not allowed in the definition of feedforward networks.

We next study multiscale BRNs whose fast subnetwork is complex balanced. This fast subnetwork can be accurately reduced using a formula for stationary moments given later, Eq (19), which is valid even in the presence of conservation laws (see Methods for details) [61, 62]. We illustrate this with an example of a transcriptional negative feedback loop (Fig 5 and Table 3), where the transcription of mRNA (M) occurs proportionally to active promoter (D_A) and then M is translated into protein (P), which promotes the production of the repressor (R). The repressor reversibly binds with D_A to form repressed promoter complex (D_R), thus completing a transcriptional negative feedback loop. Since this model can generate oscillations, it has been widely used to study circadian rhythms [66–70].

When binding and unbinding reactions are fast, D_A, D_R and R become fast species. Among slow reactions, the transcription depends on the states of fast species D_A, and thus we need to derive the QSS of the propensity function, $\alpha_M X_{D_A}$ for the reduction. The exact QSS can be

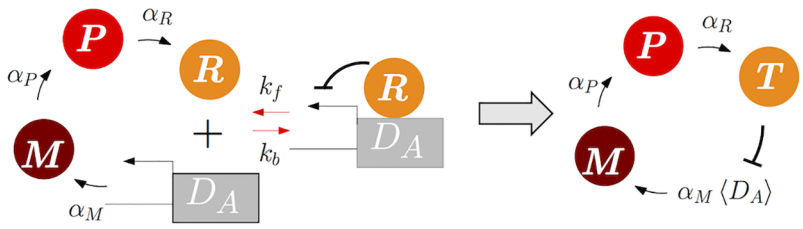

Fig 5. Model diagram of a genetic oscillator with a fast reversible binding. In the diagram of the full model (left), red arrows indicate the fast reversible binding and unbinding reactions. Note that the fast species R, D_A and their complex form a complex balanced network. In the diagram of the reduced model (right), which consists solely of slow species and reactions, $\langle D_A \rangle$ represents the conditional moment $\langle X_{D_A} | X_T \rangle$, where $X_T = X_R + X_{D_R}$. In both of the diagrams, degradation reactions are not shown, for simplicity.

https://doi.org/10.1371/journal.pcbi.1005571.g005

derived since the subnetwork of fast species with a following fast reversible binding is a complex balanced network as described in Eq (S1) (see S1 Appendix for details):

$$D_A + R \underset{k_b}{\overset{k_f}{\rightleftharpoons}} D_R. \tag{8}$$

Note that there is a conservation law as the total number of promoter ($X_{D_T} := X_{D_A} + X_{D_R}$) is conserved. Furthermore, the total repressor species ($X_T := X_R + X_{D_R}$) is a slow species as it is not affected by the fast binding and unbinding reactions (i.e. the fast binding and unbinding reactions in R and D_R are canceled). As T evolves slowly, although T is not constant on a slow timescale, it can be treated as constant or conserved on a fast timescale. Thus, on a fast timescale when slow species are treated as constant, the complex balanced network Eq (8) obeys two conservation laws: $D_T = D_A + D_R$ and $T = R + D_R$. For such a complex balanced network with conservations, we can derive the stationary conditional moment of any species using Eq (19). In particular, when $p = X_{D_T} = 10$ and $n = X_T$, our code based on Eq (19) and Eq (S3) derives $\langle X_{D_A} | X_T \rangle$ as follows (see S1 Appendix for details).

$$\begin{aligned}
\langle X_{D_A} | X_T \rangle &= f(X_T)/g(X_T). \\
f(X_T) &= 10 + 2.58274 \cdot 10^{16} X_T - 7.04208 \cdot 10^{16} {X_T}^2 + 7.62519 \cdot 10^{16} {X_T}^3 \\
&\quad -4.36905 \cdot 10^{16} {X_T}^4 + 1.46859 \cdot 10^{16} {X_T}^5 - 2.99466 \cdot 10^{15} {X_T}^6 \\
&\quad +3.64482 \cdot 10^{14} {X_T}^7 - 2.43525 \cdot 10^{13} {X_T}^8 + 6.87195 \cdot 10^{11} {X_T}^9, \\
g(X_T) &= 1 - 3.72234 \cdot 10^{17} X_T + 1.0559 \cdot 10^{18} {X_T}^2 - 1.21071 \cdot 10^{18} {X_T}^3 \\
&\quad +7.50742 \cdot 10^{17} {X_T}^4 - 2.81072 \cdot 10^{17} {X_T}^5 + 6.65138 \cdot 10^{16} {X_T}^6 \\
&\quad -1.00206 \cdot 10^{16} {X_T}^7 + 9.32029 \cdot 10^{14} {X_T}^8 - 4.87908 \cdot 10^{13} {X_T}^9 \\
&\quad +1.09951 \cdot 10^{12} {X_T}^{10}
\end{aligned}$$

By substituting this QSS of the propensity function into $\alpha_M X_{D_A}$, we can derive a reduced model (Fig 5), which is referred to as the EMB model for this example. On the other hand, previous studies used the deterministic QSS as an approximation [48, 49]:

$$\langle X_{D_A} | X_T \rangle \approx \frac{(X_{D_T} - X_T - \Omega/K + \sqrt{(X_{D_T} - X_T - \Omega/K)^2 + 4\Omega/K})}{2}.$$

By substituting this approximating moment for X_{D_A}, we can derive another reduced model, which is referred to as the AMB model for this example. The deterministic QSS used in the

Table 3. Reactions and propensity functions in the genetic oscillator (Fig 5).

Reactions	Propensity functions
$D_A \xrightarrow{\alpha_M} D_A + M$	$\alpha_M X_{D_A}$
$M \xrightarrow{\beta_M} \phi$	$\beta_M X_M$
$M \xrightarrow{\alpha_P} M + P$	$\alpha_P X_M$
$P \xrightarrow{\beta_P} \phi$	$\beta_P X_P$
$P \xrightarrow{\alpha_R} P + R$	$\alpha_R X_P$
$R \xrightarrow{\beta_R} \phi$	$\beta_R X_R$
$D_R \xrightarrow{\beta_R} D_A$	$\beta_R X_{D_R}$
$D_A + R \xrightarrow{k_f} D_R$	$\frac{k_f}{\Omega} X_{D_A} X_R$
$D_R \xrightarrow{k_b} D_A + R$	$k_b X_{D_R}$

Here $\alpha_M = 10\ h^{-1}$ and $\alpha_P = \alpha_R = \beta_M = \beta_P = \beta_R = 1\ h^{-1}$. $\frac{k_f}{\Omega} = \frac{K}{\Omega}\frac{1}{\epsilon}\ h^{-1}$ and $k_b = \frac{1}{\epsilon}\ h^{-1}$. $\frac{K}{\Omega} = \frac{10^3}{625}$ is an inverse of a dissociation constant whose unit is the number of molecules. Total number of promoter ($X_{D_T} := X_{D_A} + X_{D_R}$) is 10. Ω represents the volume of the system and $\epsilon \ll 1$.

https://doi.org/10.1371/journal.pcbi.1005571.t003

AMB model is derived with the total QSSA, which uses the new slow variable (T) to improve the accuracy of the reduction. The stochastic reduction based on the total QSSA has been known to provide more accurate approximation for the stochastic simulations of the full model than the model based on the standard QSSA (see [22, 23, 48, 49] for details). However, the EMB model provides an even more accurate approximation (Fig 6A and 6B). Specifically, both Fourier transforms and the distribution of periods of simulated trajectories with the full model is more accurately captured by the EMB model than the AMB model. The mean and standard deviation of the periods of the full model approach to those of the EMB model, but not the AMB model as the reversible binding becomes faster (i.e. ϵ decreases) (Fig 6C and 6D).

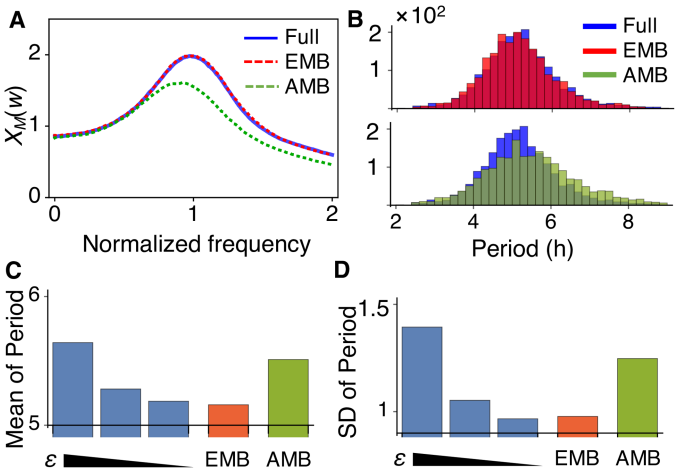

Fig 6. Period distributions of full and reduced models. (A) Fourier transforms of stochastic trajectories with about 10^4 cycles of the EMB model, the AMB model and the full model with $\epsilon = 0.1$. (B) After partitioning the trajectory of 10^4 cycles into $2{\cdot}10^3$ trajectories so that each trajectory consists of about 5 cycles, the autocorrelation of each trajectory is calculated to estimate the period of each trajectory. The period distribution of $2{\cdot}10^3$ trajectories of the EMB model (above) better captures that of the full model with $\epsilon = 0.1$ than that of the AMB model (bottom). (C-D) The mean and the standard deviation of period distributions of the EMB model, the AMB model, and the full model with $\epsilon = 10, 1, 0.1$.

https://doi.org/10.1371/journal.pcbi.1005571.g006

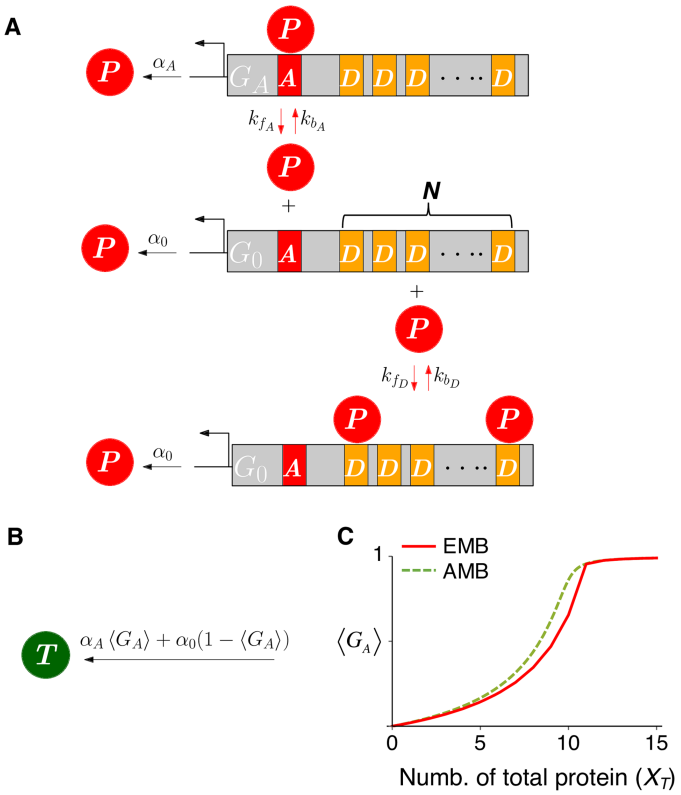

Fig 7. Model diagram of a positive feedback loop with decoys. (A) In the diagram of the full model, red arrows indicate the fast reversible binding and unbinding reactions between transcriptional factor (P) and either a regulatory promoter site (A) or one of N identical nonregulatory decoy binding sites (D). These two fast reversible bindings form a complex balanced network with species P, G_0, G_A, D, and P: D with conservations, $X_{G_0} + X_{G_1} = 1$ and $X_D + X_{P:D} = N$. (B) The reduced model consists solely of a slow species, which is the total number of transcription factors T ($X_T = X_P + X_{G_A} + X_{P:D}$). $\langle G_A \rangle$ represents stationary conditional moment, $\langle X_{G_A} | X_T \rangle$. In both of the diagrams (A and B), degradation reactions are not shown, for simplicity. (C) The exact moment $\langle X_{G_A} | X_T \rangle$, which is used for the EMB model and its approximation, which is used for the AMB model. When $X_T < N = 10$, they show a discrepancy.

https://doi.org/10.1371/journal.pcbi.1005571.g007

In summary, when fast species form a complex balanced network with conservation laws, we can find the stationary conditional moments of fast species using Eq (19) and thus derive a more accurate reduction of the stochastic system.

Reduction of a stochastic system with a coupled fast competitive bindings

Here we consider another multiscale stochastic system, a transcriptional positive feedback loop with decoys (Fig 7A and Table 4) whose fast timescale subnetwork consists of coupled competitive reversible bindings and is complex balanced. This was developed to investigate the influence of decoys on gene expression noise [71]. In the model, transcription factors (P) can bind to both a promoter site (G_0) and N identical nonregulatory decoy binding sites (D). When P is bound to the promoter site, the gene becomes active (G_A) and thus the transcriptional rate increases. While decoy is assumed to protect the transcription factor from degradation in the original model [71], here we assume that the transcriptional factor degrades equally regardless of its binding status (Table 4).

Table 4. Reactions and propensity functions in the positive feedback loop with decoys (Fig 7A).

Reactions	Propensity functions
$G_0 \xrightarrow{\alpha_0} G_0 + P$	$\alpha_0 X_{G_0}$
$G_A \xrightarrow{\alpha_A} G_A + P$	$\alpha_A X_{G_A}$
$G_0 + P \xrightarrow{k_{f_A}} G_A$	$\frac{k_{f_A}}{\Omega} X_{G_0} X_P$
$G_A \xrightarrow{k_{b_A}} G_0 + P$	$k_{b_A} X_{G_A}$
$D + P \xrightarrow{k_{f_D}} D:P$	$\frac{k_{f_D}}{\Omega} X_D X_P$
$D:P \xrightarrow{k_{b_D}} D + P$	$k_{b_A} X_{D:P}$
$P \xrightarrow{\beta_P} \phi$	$\beta_P X_P$
$D:P \xrightarrow{\beta_P} D$	$\beta_P X_{D:P}$
$G_A \xrightarrow{\beta_P} G_0$	$\beta_P X_{G_A}$

Here $\alpha_0 = 4\ m^{-1}$, $\alpha_A = 10\ m^{-1}$ (Fig 8A and 8B) or $\alpha_0 = 8\ m^{-1}$, $\alpha_A = 20\ m^{-1}$ (Fig 8C and 8D). $\frac{k_{f_A}}{\Omega} = 2000\ m^{-1}$, $k_{b_A} = 100\, m^{-1}$, $\frac{k_{f_D}}{\Omega} = 10000\ m^{-1}$, $k_{b_D} = 100\, m^{-1}$, $\beta_P = 0.8\ m^{-1}$. Total number of promoter ($X_{G_0} + X_{G_A}$) is 1. Total number of decoy sites (N: = $X_D + X_{D:P}$) is 10. Ω represents the volume of the system.

https://doi.org/10.1371/journal.pcbi.1005571.t004

Because reversible bindings between P and G_0 or D are faster than other reactions, the following competitive bindings form the fast timescale subnetwork.

$$G_0 + P \underset{k_{b_A}}{\overset{k_{f_A}}{\rightleftharpoons}} G_A$$

$$D + P \underset{k_{b_D}}{\overset{k_{f_D}}{\rightleftharpoons}} D:P$$

This subnetwork is a complex balanced network as described in Eq (S4) in S1 Appendix. This network obeys two conservation laws: total gene number ($X_{G_0} + X_{G_A}$) and total decoy sites ($X_D + X_{D:P}$) are 1 and 10, respectively. Furthermore, total transcriptional factors (T: = $P + G_A + D$: P) slowly evolve as they are not affected by fast binding and unbinding reactions. Thus, on a fast timescale, T can be treated as a constant or conserved. Since this is a complex balanced network, we can use Eq (19) to derive any of the stationary moments, subject to the three conservations. In particular, Eq (S6) in S1 Appendix with $n_A = X_T$ and $n_C = X_D + X_{D:P} = 10$ yields $\langle X_{G_A} | X_T \rangle$, which can be calculated with the code provided in this work (Fig 7C). This derives the exact QSS of slow propensity functions, $\alpha_P X_{G_A}$ and $\alpha_0 X_{G_0} = \alpha_0 (1 - X_{G_A})$, describing the production of the slow species T: $\alpha_A \langle X_{G_A} | X_T \rangle$ and $\alpha_0 (1 - \langle X_{G_A} | X_T \rangle)$. By using the exact QSS, the reduced model, which is solely determined by the slow species T can be derived (Fig 7B). This reduced model is referred to as the EMB model for this example. On the other hand, the previous study [71] used the following approximate moment:

$$\langle X_{G_A} | X_T \rangle \approx \frac{(X_T - K_D/\Omega - N + \sqrt{(X_T - K_D/\Omega - N)^2 + 4K_D X_T/\Omega})}{2K_A/\Omega + (X_T - K_D/\Omega - N + \sqrt{(X_T - K_D/\Omega - N)^2 + 4K_D X_T/\Omega})}, \quad (9)$$

where $K_D = k_{b_D}/k_{f_D}$ and $K_A = k_{b_A}/k_{f_A}$. The reduced model based on this approximate moment is referred to as the AMB model for this example. The previous study found that the accuracy of the AMB model decreases as the decoy binding becomes tighter (i.e. smaller K_D) [71]. Thus,

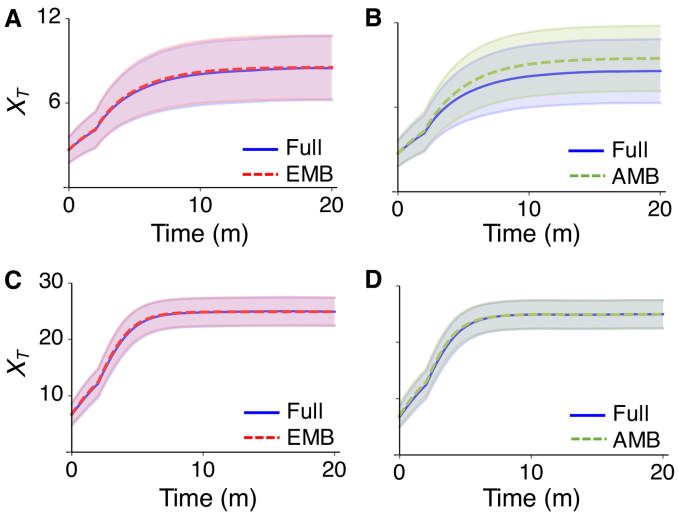

Fig 8. Trajectories of the full model, the EMB model and the AMB model of the positive feedback loop with decoys. (A-B) The lines and colored ranges represent $E(X_T)$ and $E(X_T) \pm SD(X_T)/2$ of 10^4 stochastic simulations when $\alpha_A = 10$ and $\alpha_0 = 4$. Here $X_i(0) = 0$. (C-D) When $\alpha_A = 20$ and $\alpha_0 = 8$, so that overall X_T is greater than the total number of decoy sites (i.e $N = 10$), the AMB model also becomes accurate.

https://doi.org/10.1371/journal.pcbi.1005571.g008

we investigated whether the EMB model can provide an accurate approximation even when the K_D is small. Despite the small value of K_D, the EMB model provides an accurate approximation in contrast to the AMB model (Fig 8A and 8B). This describes that the inaccuracy of the AMB model when K_D is small stems from the inaccuracy of the approximate moment Eq (9). Indeed, when we compared the exact moment and the approximate moment (Fig 7C), we characterized the discrepancy between them. In particular, the discrepancy mainly occurs when T is less than the total number of decoy sites (i.e. 10). Thus, we hypothesized that the accuracy of the AMB model increases as T increases. To investigate this, we increased the transcription rates α_A and α_0 so that overall level of T increases. In this case, the accuracy of the AMB model considerably increases (Fig 8C and 8D). This indicates that by comparing the exact moment and the approximate moment, we can find validity conditions for the AMB model and thus when the stochastic analysis based on the approximation Eq (9) in the previous study [71] is valid (e.g. when $T \gg N$).

Discussion

Stochastic multiscale BRNs can be reduced by replacing the fast species with their QSS, which accelerates stochastic simulations. For the reduction, approximate QSS of fast species are frequently used in the presence of nonlinear reactions [8, 14–27]. However, the validity conditions for such approximations have not been fully understood or are often difficult to test [45–50]. In this work, we have demonstrated that a fairly large class of nonlinear BRNs can be reduced by deriving the exact QSS of fast species rather than the approximate QSS even in the presence of nonlinear reactions. Specifically, when fast species constitute either a feedforward network or a complex balanced network with conservations, their exact QSS can be derived using our computational packages based on the Eq (15), Eq (S3), or Eq (S6) (S1 Appendix) [60, 62]. Reduced models in this way accurately approximate the stochastic dynamics of the original full models as long as disparate timescales exist (Figs 2, 4, 6 and 8).

As complex balanced networks with conservations include various types of reversible bindings, they are frequently observed as a fast subnetwork of gene regulatory networks where fast

bindings occur between molecules such as transcriptional factors and RNA polymerase and regulatory or non-regulatory sites of genes [57]. Complex balanced networks are also embedded in many signalling networks such as receptor-ligand signal pathways in response to various stimuli such as heat [26, 72], inflammation [73], and blood glucose [74]. Furthermore, a feedforward network is one of fundamental motifs of gene and protein regulatory networks [64, 65]. Interestingly, a feedforward network is also observed in the networks of neuronal cells where stochastic multiscale dynamics of ion channels exist [75–78]. Extension of our work to such multiscale stochastic neuronal networks would be an interesting direction for future work. Another interesting future work would be to investigate other classes of nonlinear BRNs whose exact moments can be derived. In particular, our computational package, FEEDME can be used to derive the exact moment for any BRNs which have linear moment closure property as well as the feedforward network.

Various approximation schemes for the QSS of fast species have been usually tested by comparing the simulated distributions or trajectories of a reduced model and an original full model [8, 14–27]. Such a test is computationally expensive because it requires stochastic simulations of a multiscale full model for many times. Such high computational cost is prohibitive when testing the accuracy of the approximation for complex examples or a wide range of parameters. On the other hand, if an exact QSS is known, the accuracy of the approximation can be tested easily by comparing the exact QSS and the approximate QSS as seen in Fig 7C. Furthermore, in this way, we can understand more intuitively under which conditions the approximation becomes accurate or not (Fig 8). Thus, non-linear feedforward networks or complex balanced networks can be an effective test platform for various approximate schemes such as normal or log-normal moment closure [52].

Methods

Chemical master equation

A BRN consists of a finite set of reactions $\mathcal{R} = \{R_j, j = 1, 2, \ldots, m\}$ acting on species, $\mathcal{S} = \{S_i,\ i = 1, 2, \ldots n\}$. By defining

$$S_i(t) = \text{ the number of species } S_i \text{ at time } t$$

we can denote the probability that the state of the system, $S = (S_1, \ldots, S_n)'$ equals $k = (k_1, \ldots, k_n) \in \mathbb{Z}^n_{\geq 0}$ at t as

$$p_k(t) = \mathbb{P}[S(t) = k].$$

For reactions,

$$R_j : \quad \sum_{i=1}^{n} a_{ij} S_i \longrightarrow \sum_{i=1}^{n} b_{ij} S_i, \quad j \in \{1, 2, \ldots, m\}, \tag{10}$$

where a_{ij} and b_{ij} are *stoichiometry coefficients*, their stochastic behaviors are described by propensity functions:

$$\rho_j : \mathbb{Z}^n_{\geq 0} \to \mathbb{R}_{\geq 0}, \quad j = 1, \ldots, m, \text{ with } \rho_j(0) = 0$$

Specifically, $\rho_j(k_1, \ldots, k_n)dt$ is the probability that reaction R_j takes place, in a short interval of length dt, provided that the complete state was $S = (k_1, \ldots, k_n)$ at the beginning of the interval. Mass action kinetics based on collision theory assumes that the propensity function is proportional to the number of ways in which species can combine to form the jth source complex (see [79]) when temperature and volume are constant, and the system is well-

mixed:

$$\rho_j(k) = \kappa_j \prod_{i=1}^{n} \binom{k_i}{a_{ij}} \quad j = 1, \ldots, m. \tag{11}$$

where $\binom{k_i}{a_{ij}}$ is the combinatorial number and is zero by definition when any $k_i < a_{ij}$. The coefficients κ_j are non-negative "kinetic constants" represents quantities related to the volume, shapes of the reactants, chemical and physical information, and temperature. In particular, $\kappa_j = \frac{\kappa'_j}{\Omega^{\sum_{i=1}^{n} a_{ij}-1}}$ when κ'_j is macroscopic reaction rate in terms of concentration and Ω is the volume of system.

Using the propensity functions, we can derive a *Chemical Master Equation (CME)*, which is the differential form of the Chapman-Kolmogorov forward equation for $p_k(t)$:

$$\frac{dp_k}{dt} = \sum_{j=1}^{m} \rho_j(k - \gamma_j)\, p_{k-\gamma_j} - \sum_{j=1}^{m} \rho_j(k)\, p_k\,, \quad k \in \mathbb{Z}^n_{\geq 0} \tag{12}$$

where γ_j is a vector whose ith component is b_{ji}–a_{ji}, which represents the net change in the number of S_i each time that R_j occurs. Note that the propensity function ρ_j has the property that $\rho_j(k-\gamma_j) = 0$ unless $k \geq \gamma_j$ (coordinatewise inequality). There is one equation for each $k \in \mathbb{Z}^n_{\geq 0}$, so this is an infinite system of linked equations. When discussing the CME, we will assume that an initial probability vector $p(0)$ has been specified, and that there is a unique solution of Eq (12) defined for all $t \geq 0$. We do not discuss existence and uniqueness results, which are subtle. See [80] for details.

Feedforward networks

Derivatives of moments are expressed as linear combinations of moments. Here, we review how to derive equations for derivatives of moments with arbitrary orders using simple algebra of polynomials. First, note that each rate $\rho_j(k)$ as in Eq (11) can be expanded into a polynomial in which each variable k_i has an exponent less or equal to a_{ij} for suitably redefined coefficients κ_{c_j}'s:

$$\rho_j(k) = \sum_{c_j \leq a_j} \kappa_{c_j} k^{c_j}, \tag{13}$$

where $k^{c_j} = k_1^{c_{1j}} \ldots k_n^{c_{nj}}$ and "$\leq$" is understood coordinatewise. For a monomial function $M : \mathbb{Z}^n_{\geq 0} \to \mathbb{R}$:

$$M(k) = k^u = k_1^{u_1} k_2^{u_2} \ldots k_n^{u_n},$$

the expectation of the random variable $M(S)$ is

$$\mathbb{E}[M(S(t))] = \sum_{k \in \mathbb{Z}^n_{\geq 0}} p_k(t)\, M(k)\,,$$

since $p_k(t) = \mathbb{P}[S(t) = k]$. After taking the derivative of this equation and substituting CME Eq (12) to $\frac{dp_k}{dt}$, the following can be derived (see [81] for more details):

$$\frac{d}{dt}\mathbb{E}[M(S(t))] = \sum_{j=1}^{m} \mathbb{E}\Big[\rho_j(S(t))\, \Delta_{\gamma_j, M}(S(t))\Big], \tag{14}$$

where $\Delta_{\gamma_j, M}(k) := M(k + \gamma_j) - M(k)$. For instance,

$$\Delta_{(1,0),k_1^2k_2}(k_1, k_2) = (k_1 + 1)^2 k_2 - k_1^2 k_2 = 2k_1 k_2 + k_2.$$

Note that $k_1^2 k_2$ is canceled. Such cancelation in $M(k + \gamma_j) - M(k)$ leads to

$$\Delta_{\gamma_j, M}(k) = \sum_{v \in \mathcal{I}(u,j)} d_v k^v$$

for appropriate coefficients d_v, where

$$\mathcal{I}(u,j) := \left\{ v \in \mathbb{Z}^n_{\geq 0} \,\middle|\, \begin{array}{c} v = u - \mu,\ u \geq \mu \neq 0 \\ \mu_i = 0 \text{ for each } i \text{ such that } \gamma_{ij} = 0 \end{array} \right\}.$$

Combining this with Eq (13), the derivative of the moment of order $u = (u_1, \ldots, u_n)$ can be described as a linear combination of other moments $(v + c_j)$:

$$\frac{d}{dt}\mathbb{E}[S(t)^u] = \sum_{j=1}^{m} \sum_{c_j \leq a_j} \sum_{v \in \mathcal{I}(u,j)} d_v \kappa_{c_j} \mathbb{E}\left[S(t)^{v+c_j}\right]. \tag{15}$$

To solve this equation, we need to know all $\mathbb{E}[S(t)^{v+c_j}]$, which typically results in an infinite set of coupled linear ordinary differential equations of moments. Often, for given a particular moment of order u of interest, there is a finite set of moments, including the desired one, that satisfies a finite set of differential equations (i.e. *linear moment closure*). Specifically, a given moment of order u is under linear moment closure when there exist $x(t) = \{u_1, \ldots, u_N\}$, where $u_1 = u$, and $A \in \mathbb{R}^{N \times N}$ such that $\dot{x}(t) = Ax(t)$ for all $t \geq 0$. The matrix A can be identified using Eq (15) recursively. It is well known that if all reactions have order 0 or 1, any moments are under a linear moment closure. Recent work found that such linear moment closure can be obtained for more general class of models such as nonlinear feedforward networks or some non-feedforward networks with conservations laws [60].

Linear moment closure property of feedforward network. A BRN is a *feedforward network* if its n species can be partitioned into p layers, in such a way that each reaction whose order is higher than one and involves species in layer π must have the form:

$$a_{i_1 j} S_{i_1} + \ldots a_{i_q j} S_{i_q} \quad \longrightarrow \quad a_{i_1 j} S_{i_1} + \ldots a_{i_q j} S_{i_q} + b_{i_{q+1} j} S_{i_{q+1}} + \ldots b_{i_{q+q'} j} S_{i_{q+q'}}$$

where all the species $S_{i_1}, \ldots, S_{i_q}$ belong to layers having indices $<\pi$, and the species $S_{i_{q+1}}, \ldots, S_{i_{q+q'}}$ are in layer π. In other words, multimers of species in "previous" layers can "catalyze" the production of species in the given layer, but are not affected by these reactions. This can be summarized by saying that for reactions at any given layer π, the only species that appear as reactants in nonlinear reactions are those in layers $<\pi$ and the only ones that can change are those in layer π.

It was shown in [60] that given any desired moment u of the feedforward network, there is a finite linear differential equation $\dot{x}(t) = Ax(t)$ for a suitable set of N moments

$$x(t) := (\mathbb{E}[S^{u_1}(t)], \ldots, \mathbb{E}[S^{u_N}(t)])',$$

which contains the moment u of interest. In practice, we simply compute Eq (15) starting from a desired moment, then recursively apply the same rule to the moments newly appearing in the right-hand side, and so forth until no new moments appear. The integer N at which the system closes might be very large, but the procedure is guaranteed to stop. An estimation of the integer N can be done based on the solution of a linear program whose

structure depends on the network. This is discussed in detail in [60]. To help performing this recursive calculation, we provide a computational package, FEEDME (FEEDforward Moment Equations) in this work. Then, the stationary moments can be computed by simply solving $Ax = 0$, which allows for the reduction of multi-scale feedforward network. For instance, the example in Fig 3 requires, for the computation of the conditional second moment of R, the following moments ($N = 24$): 0002, 0001, 0110, 0111, 0010, 0011, 0220, 1100, 1101, 0020, 0100, 0101, 0120, 0210, 1000, 1001, 1200, 1210, 0200, 1010, 1110, 2200, 2000, 2100, where we are using the convention that the string "*ijkl*" represents the expectation of $E^i F^j Q^k R^l$. (The sample FEEDME.m script produces this output). The highest-order moments have order 4 (0220 and 2200). We also remark that non-feedforward networks also lead to the linear moment closure, provided that conservation laws ensure that variables appearing on nonlinear reactions take only a finite set of possible values (see [60]). Note that FEEDME can be used to derive moment equations for any BRNs who have linear moment closure property as well as the feedforward network.

Complex balanced networks

Stationary moments of complex balanced networks with conservations. The large volume or thermodynamic limit of the CME is a deterministic system [82, 83]. For this associated deterministic network, a steady state $\bar{\lambda} \in \mathbb{R}^n_{>0}$ is complex-balanced if, *for each individual* complex $c \in \mathcal{C}$, the rate at which c is produced is equal to the rate at which it is consumed; i.e., outflows of c and inflows of c balance out.

Foundational results in deterministic complex balanced network theory were obtained by Horn, Jackson, and Feinberg (see [84, 85]). One of the key theorems is that a complex balanced steady state exists if the network is *weakly reversible* and have *deficiency zero*. Weak reversibility means that each connected component of the reaction graph must be strongly connected (i.e. if there is a direct path from a component to another, the vice versa is true). The deficiency is computed as $n_c - \ell - r$, where n_c is the number of complexes, r is the rank of the matrix Γ, and ℓ is the number of "linkage classes" (connected components of the reaction graph). One of the most interesting features of this theorem is that no assumption needs to be made about the kinetic constants (Of course, the steady state will depend on kinetic constants). We refer the reader to the citations for details on deficiency theory, as well as, of interest in the present context, several examples discussed in [62]. The theorems for weakly reversible deficiency zero networks are actually far stronger, and they show that *every* possible steady state of the corresponding deterministic network is complex balanced, and also that they are asymptotically stable relative to stoichiometry classes.

The connection between the deterministic complex balanced steady state and the solutions of steady state CME (ssCME) was a beautiful observation made in [61], but can be traced to the "nonlinear traffic equations" from queuing theory, described in Kelly's textbook [86], Chapter 8 (see also [87] for a discussion). Specifically, when the steady state vector, $\bar{\lambda} \in \mathbb{R}^n_{>0}$ is complex-balanced,

$$\Pi = \left\{ p_k = \frac{\bar{\lambda}^k}{k!} \ , \ \ k \in \mathbb{Z}^n_{\geq 0} \right\} \tag{16}$$

becomes a solution of the ssCME equations. The elements of Π add up to:

$$\sum_{k \in \mathbb{Z}^n_{\geq 0}} p_k = \sum_{k_1=0}^{\infty} \cdots \sum_{k_n=0}^{\infty} \frac{\bar{\lambda}_1^k}{k_1!} \cdots \frac{\bar{\lambda}_n^k}{k_n!} = Z := e^{\bar{\lambda}_1} \ldots e^{\bar{\lambda}_n}$$

Thus, normalizing by the total, $\{p_k/Z, k \in \mathbb{Z}^n_{\geq 0}\}$ is a probability distribution satisfying the ssCME equations. The interpretation of this solution is that at the steady state, S_i, $i = 1, \ldots, n$ are n independent Poisson random variables with parameters $\bar{\lambda}_i$ respectively, so

$$\mathbb{P}[S_1 = k_1, S_2 = k_2, \ldots, S_n = k_n] \;=\; e^{-(\bar{\lambda}_1+\ldots+\bar{\lambda}_n)} \frac{\bar{\lambda}_1^{k_1}}{k_1!}\frac{\bar{\lambda}_2^{k_2}}{k_2!}\cdots\frac{\bar{\lambda}_n^{k_n}}{k_n!} \tag{17}$$

for $k \geq 0$ (and zero otherwise). Next, let's consider the case when the network satisfies additional stoichiometric constraints of the network (e.g. conservation laws):

$$Y_j := \sum_{i=1}^{n} \alpha_{ji} S_i = \beta_j \quad , \quad j = 1, \ldots, q\,. \tag{18}$$

Observe that

$$\begin{aligned} &\mathbb{P}\left[Y_1 = \beta_1, \ldots, Y_q = \beta_q\right] \\ = &\sum_{\substack{k_1,\ldots,k_n \geq 0 \\ \alpha_{11}k_1+\ldots+\alpha_{1n}k_n = \beta_1,\ \ldots,\ \alpha_{q1}k_1+\ldots+\alpha_{qn}k_n = \beta_q}} e^{-(\bar{\lambda}_1+\ldots+\bar{\lambda}_n)} \frac{\bar{\lambda}_1^{k_1}}{k_1!}\frac{\bar{\lambda}_2^{k_2}}{k_2!}\cdots\frac{\bar{\lambda}_n^{k_n}}{k_n!} \\ =: \;& e^{-(\bar{\lambda}_1+\ldots+\bar{\lambda}_n)} Z(\beta_1, \ldots, \beta_q)\,, \end{aligned}$$

where $Z(\beta_1, \ldots, \beta_q)$ is referred to as the partition function. This leads to the following conditional probability at the steady state if k satisfies the stochiometric constrains:

$$\mathbb{P}[S_1 = k_1, S_2 = k_2, \ldots, S_n = k_n \,|\, Y_1 = \beta_1, \ldots, Y_m = \beta_m] \;=\; \frac{1}{Z(\beta_1, \ldots, \beta_q)} \frac{\bar{\lambda}_1^{k_1}}{k_1!}\frac{\bar{\lambda}_2^{k_2}}{k_2!}\cdots\frac{\bar{\lambda}_n^{k_n}}{k_n!}$$

and is zero otherwise. If our interest is in computing this conditional probability, the main effort goes into computing the partition function, $Z(\beta_1, \ldots, \beta_q)$. The main contribution of the paper [62] was to provide effective algorithms for the computation of $Z(\beta_1, \ldots, \beta_q)$ recursively on the β_i's. A package for that purpose, called MVPoisson, was included with that paper.

Importantly, the stationary conditional moment of any species at the steady state can be obtained using the following formula:

$$E[S_j^r, | \, Y] \;=\; \bar{\lambda}_j \cdot \frac{Z(\beta_1 - r\alpha_{1j}, \beta_2 - r\alpha_{2j}, \ldots, \beta_q - r\alpha_{qj})}{Z(\beta_1, \ldots, \beta_q)} \tag{19}$$

when all $\beta_i \geq \alpha_{ij}$, and zero otherwise. Mixed moments can be also calculated using the partition function [62]. Thus, as long as the participation can be calculated, any desired stationary moments can be derived and thus model can be accurately reduced.

Summary of the procedure to derive stationary moments of complex balanced networks.

Step 1. Check whether the given network is complex balanced, which can be done by checking deficiency and weak reversibility of the network.

Step 2. Find all conservation laws, which can be done by finding the left nullspace of the stoichiometry matrix.

Step 3. Choose any steady state vector $\bar{\lambda} \in \mathbb{R}^n_{>0}$ of the deterministic system describing the network (usually a simple one).

Step 4. For the choice of $\bar{\lambda} \in \mathbb{R}^n_{>0}$, derive the partition function with the stoichiometric constraints given by the conservation laws.

Step 5. Calculate the partition function by rewriting the sum of the partition function with minimal indices using the conservation laws, using the algorithm described in S1 Appendix. Alternatively, such calculation can be done by deriving the recursion relations among partition functions with the MVPoisson package [62].

Step 6. Calculate the desired stationary moments using Eq (19).

Detailed description of this procedure is illustrated in S1 Appendix using the examples of Figs 5 and 7.

Supporting information

S1 Appendix. Detailed illustration of the procedure to derive stationary moments of complex balanced networks.
(PDF)

Author Contributions

Conceptualization: JKK EDS.

Formal analysis: JKK EDS.

Funding acquisition: JKK EDS.

Investigation: JKK EDS.

Methodology: JKK EDS.

Project administration: JKK EDS.

Software: JKK EDS.

Supervision: JKK EDS.

Validation: JKK EDS.

Visualization: JKK EDS.

Writing – original draft: JKK EDS.

Writing – review & editing: JKK EDS.

References

1. Ghaemmaghami S, Huh WK, Bower K, Howson RW, Belle A, Dephoure N, et al. Global analysis of protein expression in yeast. Nature. 2003; 425(6959):737–41. https://doi.org/10.1038/nature02046 PMID: 14562106
2. Ishihama Y, Schmidt T, Rappsilber J, Mann M, Hartl FU, Kerner MJ, et al. Protein abundance profiling of the Escherichia coli cytosol. BMC genomics. 2008; 9(1):102. https://doi.org/10.1186/1471-2164-9-102 PMID: 18304323
3. Biggin MD. Animal transcription networks as highly connected, quantitative continua. Developmental cell. 2011; 21(4):611–626. https://doi.org/10.1016/j.devcel.2011.09.008 PMID: 22014521
4. Gillespie DT. Exact Stochastic Simulation of Coupled Chemical Reactions. The Journal of Physical Chemistry. 1977; p. 2340–2361. https://doi.org/10.1021/j100540a008

5. El Samad H, Khammash M, Petzold L, Gillespie D. Stochastic modelling of gene regulatory networks. International Journal of Robust and Nonlinear Control. 2005; 15(15):691–711. https://doi.org/10.1002/rnc.1018
6. Gillespie DT. Stochastic simulation of chemical kinetics. Ann Rev Phys Chem. 2007; 58:35–55. https://doi.org/10.1146/annurev.physchem.58.032806.104637 PMID: 17037977
7. Van Kampen NG. Elimination of fast variables. Phys Rep. 1985; 124(2):69–160. https://doi.org/10.1016/0370-1573(85)90002-X
8. Rao CV, Arkin AP. Stochastic chemical kinetics and the quasi-steady-state assumption: Application to the Gillespie algorithm. J Chem Phys. 2003; 118(11):4999–5010. https://doi.org/10.1063/1.1545446
9. Goutsias J. Quasiequilibrium approximation of fast reaction kinetics in stochastic biochemical systems. J Chem Phys. 2005; 122(18). https://doi.org/10.1063/1.1889434 PMID: 15918689
10. Ball K, Kurtz TG, Popovic L, Rempala G. Asymptotic analysis of multiscale approximations to reaction networks. Ann Appl Probab. 2006; 16(4):1925–1961. https://doi.org/10.1214/105051606000000420
11. Peleš S, Munsky B, Khammash M. Reduction and solution of the chemical master equation using time scale separation and finite state projection. J Chem Phys. 2006; 125(20):204104. https://doi.org/10.1063/1.2397685 PMID: 17144687
12. Kan X, Lee CH, Othmer HG. A multi-time-scale analysis of chemical reaction networks: II. Stochastic systems. Journal of mathematical biology. 2016; 73(5):1081–1129. https://doi.org/10.1007/s00285-016-0980-x PMID: 26945582
13. Kim, JK, Rempala, GA, Kang, HW. Reduction for stochastic biochemical reaction networks with multi-scale conservations. ArXiv e-prints. 2017;
14. Berglund N, Gentz B. Geometric singular perturbation theory for stochastic differential equations. J Differential Equations. 2003; 191(1):1–54. https://doi.org/10.1016/S0022-0396(03)00020-2
15. Vanden-Eijnden E. Fast Communications: Numerical techniques for multi-scale dynamical systems with stochastic effects. Commun Math Sci. 2003; 1(2):385–391. https://doi.org/10.4310/CMS.2003.v1.n2.a11
16. Cao Y, Gillespie DT, Petzold LR. The slow-scale stochastic simulation algorithm. J Chem Phys. 2005; 122(1). https://doi.org/10.1063/1.1824902 PMID: 15638651
17. E W, Liu D, Vanden-Eijnden E. Nested stochastic simulation algorithm for chemical kinetic systems with disparate rates. J Chem Phys. 2005; 123(19):194107. https://doi.org/10.1063/1.2109987 PMID: 16321076
18. Haseltine EL, Rawlings JB. On the origins of approximations for stochastic chemical kinetics. J Chem Phys. 2005; 123(16):164115. https://doi.org/10.1063/1.2062048 PMID: 16268689
19. Salis H, Kaznessis YN. An equation-free probabilistic steady-state approximation: Dynamic application to the stochastic simulation of biochemical reaction networks. J Chem Phys. 2005; 123(21):214106. https://doi.org/10.1063/1.2131050 PMID: 16356038
20. Lötstedt P, Ferm L. Dimensional reduction of the Fokker-Planck equation for stochastic chemical reactions. SIAM Multiscale Model Simul. 2006; 5(2):593–614. https://doi.org/10.1137/050639120
21. Dong GQ, Jakobowski L, Iafolla MA, McMillen DR. Simplification of stochastic chemical reaction models with fast and slow dynamics. Journal of Biological Physics. 2007; 33(1):67–95. https://doi.org/10.1007/s10867-007-9043-2 PMID: 19669554
22. Barik D, Paul MR, Baumann WT, Cao Y, Tyson JJ. Stochastic simulation of enzyme-catalyzed reactions with disparate timescales. Biophys J. 2008; 95(8):3563–3574. https://doi.org/10.1529/biophysj.108.129155 PMID: 18621809
23. MacNamara S, Bersani AM, Burrage K, Sidje RB. Stochastic chemical kinetics and the total quasi-steady-state assumption: Application to the stochastic simulation algorithm and chemical master equation. J Chem Phys. 2008; 129(9). https://doi.org/10.1063/1.2971036 PMID: 19044893
24. Cotter SL, Zygalakis KC, Kevrekidis IG, Erban R. A constrained approach to multiscale stochastic simulation of chemically reacting systems. J Chem Phys. 2011; 135(9):094102. https://doi.org/10.1063/1.3624333 PMID: 21913748
25. Michelotti MD, Heath MT, West M. Binning for Efficient Stochastic Multiscale Particle Simulations. SIAM Multiscale Model Simul. 2013; 11(4):1071–1096. https://doi.org/10.1137/130908038
26. Kang HW. A multiscale approximation in a heat shock response model of E. coli. BMC Syst Biol. 2012; 6(1):143. https://doi.org/10.1186/1752-0509-6-143 PMID: 23171439
27. Herath N, Del Vecchio D. Model order reduction for Linear Noise Approximation using time-scale separation. In: Decision and Control (CDC), 2016 IEEE 55th Conference on. IEEE; 2016. p. 5875–5880.
28. Gonze D, Halloy J, Goldbeter A. Deterministic versus stochastic models for circadian rhythms. J Biol Phys. 2002; 28(4):637–653. https://doi.org/10.1023/A:1021286607354 PMID: 23345804

29. Kim JK, Jackson TL. Mechanisms that enhance sustainability of p53 pulses. PLoS One. 2013; 8(6). https://doi.org/10.1371/journal.pone.0065242 PMID: 23755198

30. Black AJ, McKane AJ. Stochastic amplification in an epidemic model with seasonal forcing. Journal of Theoretical Biology. 2010; 267(1):85–94. https://doi.org/10.1016/j.jtbi.2010.08.014 PMID: 20723547

31. Tian T, Burrage K. Stochastic models for regulatory networks of the genetic toggle switch. Proceedings of the national Academy of Sciences. 2006; 103(22):8372–8377. https://doi.org/10.1073/pnas.0507818103

32. Simpson ML, Cox CD, Sayler GS. Frequency domain analysis of noise in autoregulated gene circuits. Proceedings of the National Academy of Sciences. 2003; 100(8):4551–4556. https://doi.org/10.1073/pnas.0736140100

33. Schultz D, Lu M, Stavropoulos T, Ben-Jacob E, et al. Turning oscillations into opportunities: lessons from a bacterial decision gate. Scientific reports. 2013; 3:1668. https://doi.org/10.1038/srep01668 PMID: 23591544

34. Pedraza JM, van Oudenaarden A. Noise propagation in gene networks. Science. 2005; 307 (5717):1965–1969. https://doi.org/10.1126/science.1109090 PMID: 15790857

35. Çağatay T, Turcotte M, Elowitz MB, Garcia-Ojalvo J, Süel GM. Architecture-dependent noise discriminates functionally analogous differentiation circuits. Cell. 2009; 139(3):512–522. https://doi.org/10.1016/j.cell.2009.07.046 PMID: 19853288

36. Scott M, Ingalls B, Kærn M. Estimations of intrinsic and extrinsic noise in models of nonlinear genetic networks. Chaos: An Interdisciplinary Journal of Nonlinear Science. 2006; 16(2):026107. https://doi.org/10.1063/1.2211787 PMID: 16822039

37. Murphy KF, Balázsi G, Collins JJ. Combinatorial promoter design for engineering noisy gene expression. Proceedings of the National Academy of Sciences. 2007; 104(31):12726–12731. https://doi.org/10.1073/pnas.0608451104

38. Thattai M, Van Oudenaarden A. Intrinsic noise in gene regulatory networks. Proceedings of the National Academy of Sciences. 2001; 98(15):8614–8619. https://doi.org/10.1073/pnas.151588598 PMID: 11438714

39. Ouattara DA, Abou-Jaoude W, Kaufman M. From structure to dynamics: Frequency tuning in the p53-Mdm2 network. II Differential and stochastic approaches. J Theor Biol. 2010; 264(4):1177–1189. https://doi.org/10.1016/j.jtbi.2010.03.031 PMID: 20346959

40. Gonze D, Abou-Jaoude W, Ouattara DA, Halloy J. How Molecular Should Your Molecular Model Be? On the Level of Molecular Detail Required to Simulate Biological Networks in Systems and Synthetic Biology. Methods in Enzymology. 2011; 487:171–215. https://doi.org/10.1016/B978-0-12-381270-4.00007-X PMID: 21187226

41. Toni T, Tidor B. Combined model of intrinsic and extrinsic variability for computational network design with application to synthetic biology. PLoS Comput Biol. 2013; 9(3):e1002960. https://doi.org/10.1371/journal.pcbi.1002960 PMID: 23555205

42. Riba A, Bosia C, El Baroudi M, Ollino L, Caselle M. A combination of transcriptional and microRNA regulation improves the stability of the relative concentrations of target genes. PLoS Comput Biol. 2014; 10 (2):e1003490. https://doi.org/10.1371/journal.pcbi.1003490 PMID: 24586138

43. Dovzhenok AA, Baek M, Lim S, Hong CI. Mathematical modeling and validation of glucose compensation of the neurospora circadian clock. Biophysical journal. 2015; 108(7):1830–1839. https://doi.org/10.1016/j.bpj.2015.01.043 PMID: 25863073

44. Zhang W, Tian T, Zou X. Negative feedback contributes to the stochastic expression of the interferon-β gene in virus-triggered type I interferon signaling pathways. Mathematical biosciences. 2015; 265:12–27. https://doi.org/10.1016/j.mbs.2015.04.003 PMID: 25892253

45. Thomas P, Straube AV, Grima R. The slow-scale linear noise approximation: an accurate, reduced stochastic description of biochemical networks under timescale separation conditions. BMC Syst Biol. 2012; 6. https://doi.org/10.1186/1752-0509-6-39 PMID: 22583770

46. Thomas P, Grima R, Straube AV. Rigorous elimination of fast stochastic variables from the linear noise approximation using projection operators. Physical Review E. 2012; 86(4):041110. https://doi.org/10.1103/PhysRevE.86.041110 PMID: 23214532

47. Agarwal A, Adams R, Castellani GC, Shouval HZ. On the precision of quasi steady state assumptions in stochastic dynamics. J Chem Phys. 2012; 137(4). https://doi.org/10.1063/1.4731754 PMID: 22852595

48. Kim JK, Josić K, Bennett MR. The validity of quasi-steady-state approximations in discrete stochastic simulations. Biophys J. 2014; 107(3):783–793. https://doi.org/10.1016/j.bpj.2014.06.012 PMID: 25099817

49. Kim JK, Josić K, Bennett MR. The relationship between stochastic and deterministic quasi-steady state approximations. BMC Syst Biol. 2015; 9(1):87. https://doi.org/10.1186/s12918-015-0218-3 PMID: 26597159

50. Lawson MJ, Petzold L, Hellander A. Accuracy of the Michaelis–Menten approximation when analysing effects of molecular noise. Journal of The Royal Society Interface. 2015; 12(106):20150054. https://doi.org/10.1098/rsif.2015.0054

51. Sanft KR, Gillespie DT, Petzold LR. Legitimacy of the stochastic Michaelis-Menten approximation. IET Syst Biol. 2011; 5(1):58–69. https://doi.org/10.1049/iet-syb.2009.0057 PMID: 21261403

52. Schnoerr D, Sanguinetti G, Grima R. Approximation and inference methods for stochastic biochemical kinetics-a tutorial review. Journal of Physics A: Mathematical and Theoretical. 2016;

53. Schnoerr D, Sanguinetti G, Grima R. The complex chemical Langevin equation. The Journal of chemical physics. 2014; 141(2):07B606_1. https://doi.org/10.1063/1.4885345

54. Arányi P, Tóth J. A full stochastic description of the Michaelis-Menten reaction for small systems. Acta biochimica et biophysica; Academiae Scientiarum Hungaricae. 1976; 12(4):375–388. PMID: 613716

55. Staff P. A stochastic development of the reversible Michaelis-Menten mechanism. Journal of theoretical biology. 1970; 27(2):221–232. https://doi.org/10.1016/0022-5193(70)90139-6 PMID: 5452493

56. Levine E, Hwa T. Stochastic fluctuations in metabolic pathways. Proceedings of the National Academy of Sciences. 2007; 104(22):9224–9229. https://doi.org/10.1073/pnas.0610987104

57. Bintu L, Buchler NE, Garcia HG, Gerland U, Hwa T, Kondev J, et al. Transcriptional regulation by the numbers: models. Current opinion in genetics & development. 2005; 15(2):116–124. https://doi.org/10.1016/j.gde.2005.02.007 PMID: 15797194

58. Grima R, Schmidt DR, Newman TJ. Steady-state fluctuations of a genetic feedback loop: An exact solution. The Journal of chemical physics. 2012; 137(3):035104. https://doi.org/10.1063/1.4736721 PMID: 22830733

59. Kumar N, Platini T, Kulkarni RV. Exact distributions for stochastic gene expression models with bursting and feedback. Physical review letters. 2014; 113(26):268105. https://doi.org/10.1103/PhysRevLett.113.268105 PMID: 25615392

60. Sontag ED, Singh A. Exact moment dynamics for feedforward nonlinear chemical reaction networks. IEEE Life Sciences Letters. 2015; 1:26–29. https://doi.org/10.1109/LLS.2015.2483820

61. Anderson DF, Craciun G, Kurtz TG. Product-form stationary distributions for deficiency zero chemical reaction networks. Bulletin of Mathematical Biology. 2010; 72(8):1947–1970. https://doi.org/10.1007/s11538-010-9517-4 PMID: 20306147

62. Sontag ED, Zeilberger D. A symbolic computation approach to a problem involving multivariate Poisson distributions. Advances in Applied Mathematics. 2010; 44:359–377. https://doi.org/10.1016/j.aam.2009.08.002

63. Mélykúti B, Hespanha JP, Khammash M. Equilibrium distributions of simple biochemical reaction systems for time-scale separation in stochastic reaction networks. Journal of The Royal Society Interface. 2014; 11(97):20140054. https://doi.org/10.1098/rsif.2014.0054 PMID: 24920118

64. Mangan S, Alon U. Structure and function of the feed-forward loop network motif. Proceedings of the National Academy of Sciences. 2003; 100(21):11980–11985. https://doi.org/10.1073/pnas.2133841100

65. Tyson JJ, Novák B. Functional motifs in biochemical reaction networks. Annual review of physical chemistry. 2010; 61:219–240. https://doi.org/10.1146/annurev.physchem.012809.103457 PMID: 20055671

66. Kim JK, Forger DB. A mechanism for robust circadian timekeeping via stoichiometric balance. Molecular systems biology. 2012; 8(630):630. https://doi.org/10.1038/msb.2012.62 PMID: 23212247

67. Kim JK, Kilpatrick ZP, Bennett MR, Josić K. Molecular mechanisms that regulate the coupled period of the mammalian circadian clock. Biophys J. 2014; 106:2071–2081. https://doi.org/10.1016/j.bpj.2014.02.039 PMID: 24806939

68. Zhou M, Kim JK, Eng GWL, Forger DB, Virshup DM. A Period2 phosphoswitch regulates and temperature compensates circadian period. Molecular cell. 2015; 60(1):77–88. https://doi.org/10.1016/j.molcel.2015.08.022 PMID: 26431025

69. Kim JK. Protein sequestration versus Hill-type repression in circadian clock models. IET Systems Biology. 2016; 10:125–135(10). https://doi.org/10.1049/iet-syb.2015.0090 PMID: 27444022

70. Gotoh T, Kim JK, Liu J, Vila-Caballer M, Stauffer PE, Tyson JJ, et al. Model-driven experimental approach reveals the complex regulatory distribution of p53 by the circadian factor Period 2. Proceedings of the National Academy of Sciences. 2016; 113(47):13516–13521. https://doi.org/10.1073/pnas.1607984113 PMID: 27834218

71. Burger A, Walczak AM, Wolynes PG. Influence of decoys on the noise and dynamics of gene expression. Physical Review E. 2012; 86(4):041920. https://doi.org/10.1103/PhysRevE.86.041920

72. Scheff JD, Stallings JD, Reifman J, Rakesh V. Mathematical modeling of the heat-shock response in HeLa cells. Biophysical journal. 2015; 109(2):182–193. https://doi.org/10.1016/j.bpj.2015.06.027 PMID: 26200855

73. Gnacadja G, Shoshitaishvili A, Gresser MJ, Varnum B, Balaban D, Durst M, et al. Monotonicity of interleukin-1 receptor–ligand binding with respect to antagonist in the presence of decoy receptor. Journal of theoretical biology. 2007; 244(3):478–488. https://doi.org/10.1016/j.jtbi.2006.07.023 PMID: 17011587

74. Kubota H, Noguchi R, Toyoshima Y, Ozaki Yi, Uda S, Watanabe K, et al. Temporal coding of insulin action through multiplexing of the AKT pathway. Molecular cell. 2012; 46(6):820–832. https://doi.org/10.1016/j.molcel.2012.04.018 PMID: 22633957

75. Reigl M, Alon U, Chklovskii DB. Search for computational modules in the C. elegans brain. BMC biology. 2004; 2(1):25. https://doi.org/10.1186/1741-7007-2-25 PMID: 15574204

76. Liu Y, Li C. Stochastic resonance in feedforward-loop neuronal network motifs in astrocyte field. Journal of theoretical biology. 2013; 335:265–275. https://doi.org/10.1016/j.jtbi.2013.07.007 PMID: 23871712

77. Goldwyn JH, Shea-Brown E. The what and where of adding channel noise to the Hodgkin-Huxley equations. PLoS Comput Biol. 2011; 7(11):e1002247. https://doi.org/10.1371/journal.pcbi.1002247 PMID: 22125479

78. Bertram R, Tabak J, Teka W, Vo T, Wechselberger M. Geometric Singular Perturbation Analysis of Bursting Oscillations in Pituitary Cells. In: Mathematical Analysis of Complex Cellular Activity. Springer; 2015. p. 1–52. https://doi.org/10.1007/978-3-319-18114-1_1

79. Gillespie DT. The chemical Langevin equation. Journal of Chemical Physics. 2000; 113(1):297–306. https://doi.org/10.1063/1.481811

80. Meyn SP, Tweedie RL. Stability of Markovian processes III: Foster-Lyapunov criteria for continuous-time processes. Adv Appl Prob. 1993; 25:518–548. https://doi.org/10.1017/S0001867800025532

81. Sontag ED. Lecture Notes on Mathematical Systems Biology, Rutgers University; 2002-2015.

82. Kurtz TG. The relationship between stochastic and deterministic models for chemical reactions. J Chem Phys. 1972; 57(7):2976–2978. https://doi.org/10.1063/1.1678692

83. Gillespie DT. Deterministic limit of stochastic chemical kinetics. J Phys Chem B. 2009; 113(6):1640–1644. https://doi.org/10.1021/jp806431b PMID: 19159264

84. Feinberg M. Chemical reaction network structure and the stability of complex isothermal reactors—I. The deficiency zero and deficiency one theorems. Chemical Engr Sci. 1987; 42:2229–2268. https://doi.org/10.1016/0009-2509(87)80099-4

85. Feinberg M. The existence and uniqueness of steady states for a class of chemical reaction networks. Archive for Rational Mechanics and Analysis. 1995; 132:311–370.

86. Kelly F. Reversibility and Stochastic Networks. New York: Wiley; 1979.

87. Mairesse J, Nguyen HT. Deficiency zero Petri nets and product form. In: Franceschinis G, Wolf K, editors. Applications and Theory of Petri Nets. Springer-Verlag; 2009. p. 103–122. https://doi.org/10.1007/978-3-642-02424-5_8